Supplementary Information

Figures

Fig. 1 Comparison of polyglyceryl-6 octacaprylate (PGO) and isostearyl alcohol (ISA) in agarose microdroplet gelation.

a. Test of stability of emulsion formed by water and PGO (density: 0.997 g/mL) (right) or water and ISA (density: 0.836 g/mL) (left). The emulsion was observed at 0, 30, and 60 min after 0.5 mL of Milli-Q water (Millipore) and 0.5 mL of 3% lecithin in ISA or PGO were mixed by vortex for 1 min.

b. Aggregations of agarose gel beads in the PGO (left) and the ISA (right) emulsions.

c. Diameters of agarose gel beads formed in the PGO (white) and the ISA (grey) emulsions. Values of three independent experiments are shown as box-and-violin plots using R ggplot2 package (https://ggplot2.tidyverse.org/index.html). Rhombuses (red) and circles (black) denote their arithmetic means and outliers, respectively. Numbers of agarose gel beads used for the diameter measurement are shown in parentheses. Double asterisks indicate significant differences (Wilcoxon rank sum test, $P < 0.01$).

d. Morphology of agarose gel beads formed in the PGO (left) and the ISA (right) emulsions. Bar = 100 μm.

e. Yields of agarose gel beads with <300-μm diameter from 2 mL of agarose sol solution gelated in the PGO or the ISA emulsions. Values are shown as mean ± SD. An asterisk indicates a significant difference (n = 3, Welch's *t*-test, $P < 0.05$).

Fig. 2 Evaluation of Sol state of AGM alginate cores

By dissolving agarose shells, alginate cores in AGMs were evaluated to determine whether they were sol or gel. AGMs containing rhodamine 123-labelled alginate cores were prepared without alginate solation by EDTA. The AGMs were solated with EDTA and observed for controls (Before Heating). The AGMs were heated in the presence of EDTA or $CaCl_2$ and their core diffusions were observed (After Heating). A phase contrast image (red) and an epifluorescent rhodamine 123 image (green) are overlaid. Bars indicate 500 μm (upper panels) or 100 μm (lower panels).

Fig. 3 AGM diameters

a. AGM diameters in three independent experiments are plotted as box plots with individual data points.

b. The AGM diameters in the three experiments are also shown as histograms with estimated density functions of normal distributions.

Fig. 4 AGM cores

a. AGM core volumes in the three experiments were plotted using box plots with individual data.

b. Histograms of the AGM core volumes using linear scales with log-normal distribution curves (upper panels) and using logarithmic scales with normal distribution curves (lower panels).

Fig. 5 Number of sequence reads mapped against genome regions.

The read coverage pattern is shown as an indicator of amplification bias caused during MDA. Randomly chosen reads (3×10^5 read pairs) from SAGs were mapped to the corresponding reference genome sequences. 'Comp.' indicates the genome completeness (%) estimated using CheckM.

Fig. 6 Optimisation of *E. coli* density

A series of diluted *E. coli* cells (0 to 3.05×10^8 cell/mL of alginate mixture) were used for preparation of alginate cores. A phase contrast image (red) and an epifluorescent

SYBR Green I image (green) are overlaid, and a bar indicates 100 μm. In the panel of 3.05×10^6 cell/mL, arrows indicate *E. coli* cells.

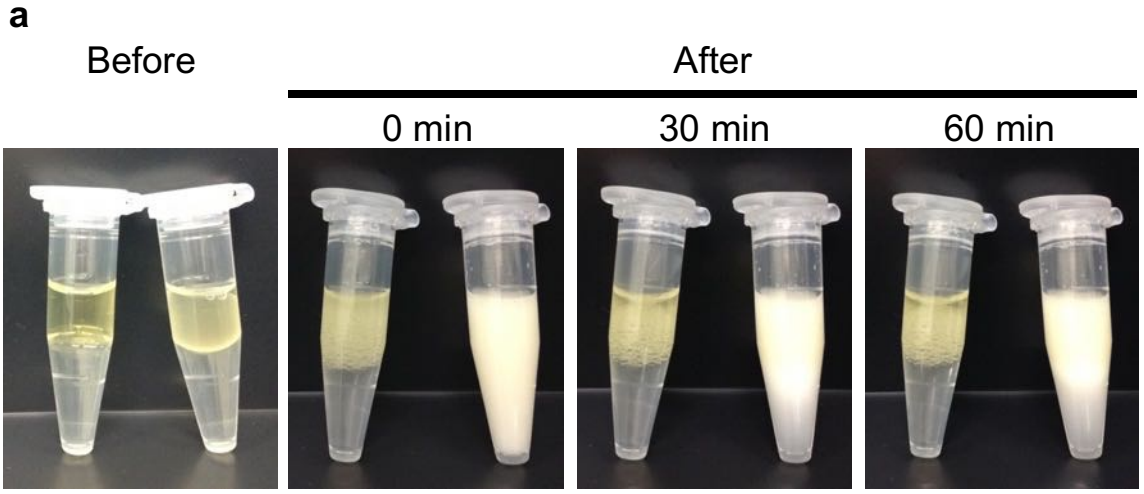
a
Before
After
0 min
30 min
60 min

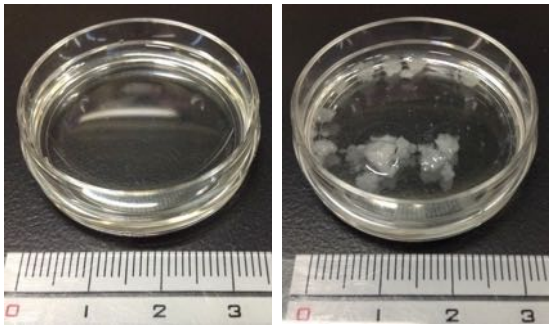
b

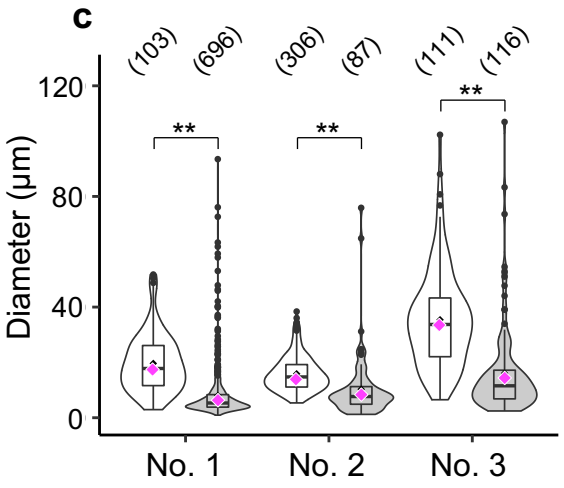
c
(103)
(696)
(306)
(87)
(111)
(116)
**
**
**
120
80
40
0
Diameter (μm)
No. 1
No. 2
No. 3

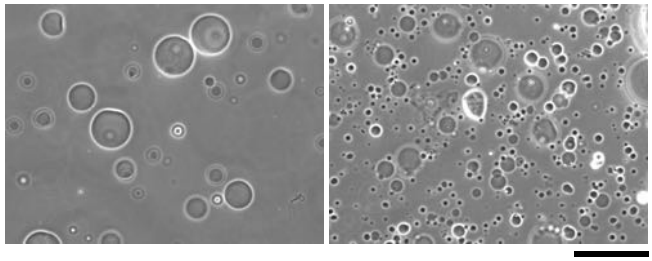
d

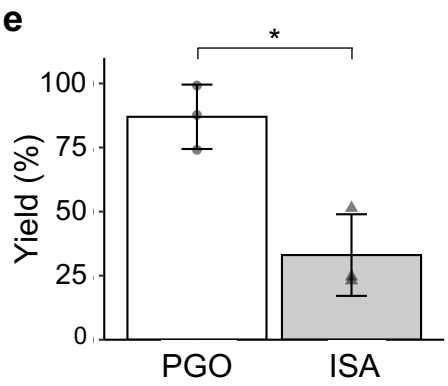
e
*
100
75
50
25
0
Yield (%)
PGO
ISA

Fig. 1

58

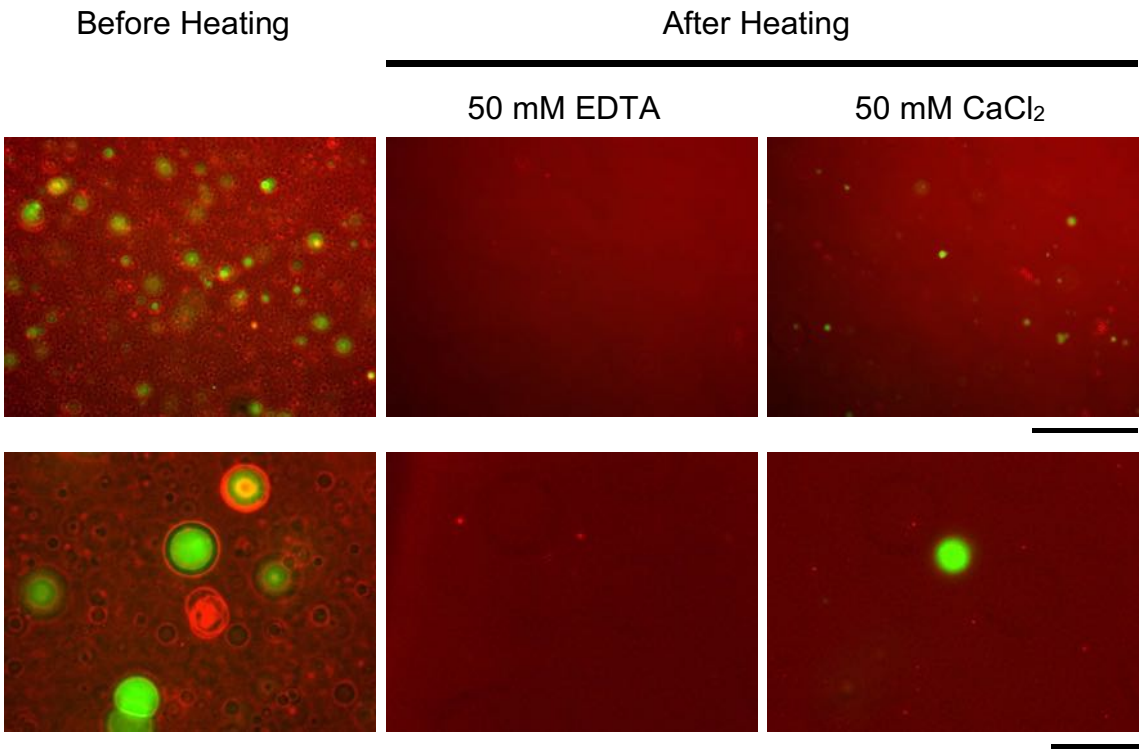

Fig. 2

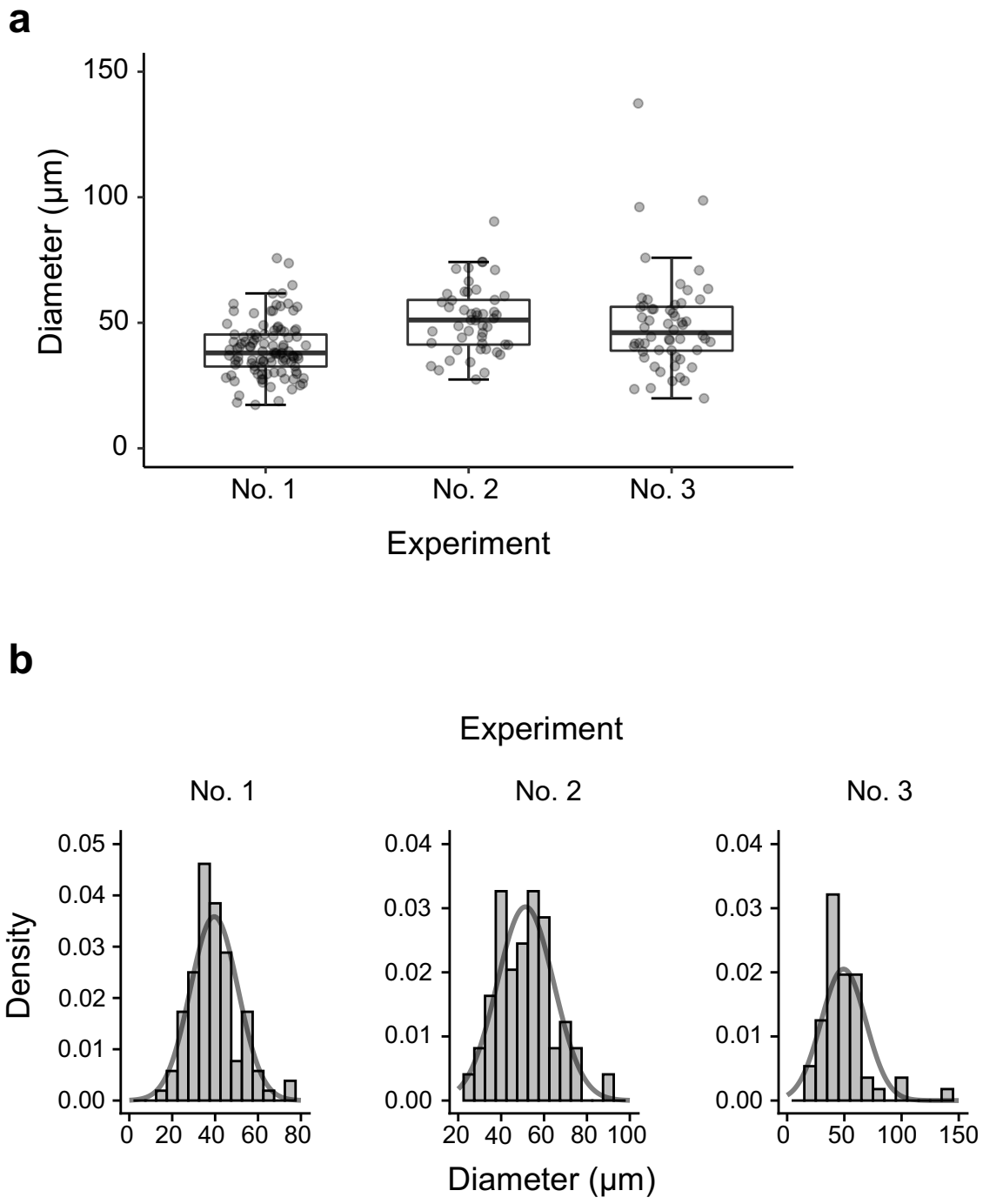
a
150
100
50
0
Diameter (μm)
No. 1
No. 2
No. 3
Experiment
b
Experiment
No. 1
No. 2
No. 3
Density
0.05
0.04
0.03
0.02
0.01
0.00
0
20
40
60
80
100
50
150
Diameter (μm)

Fig. 3

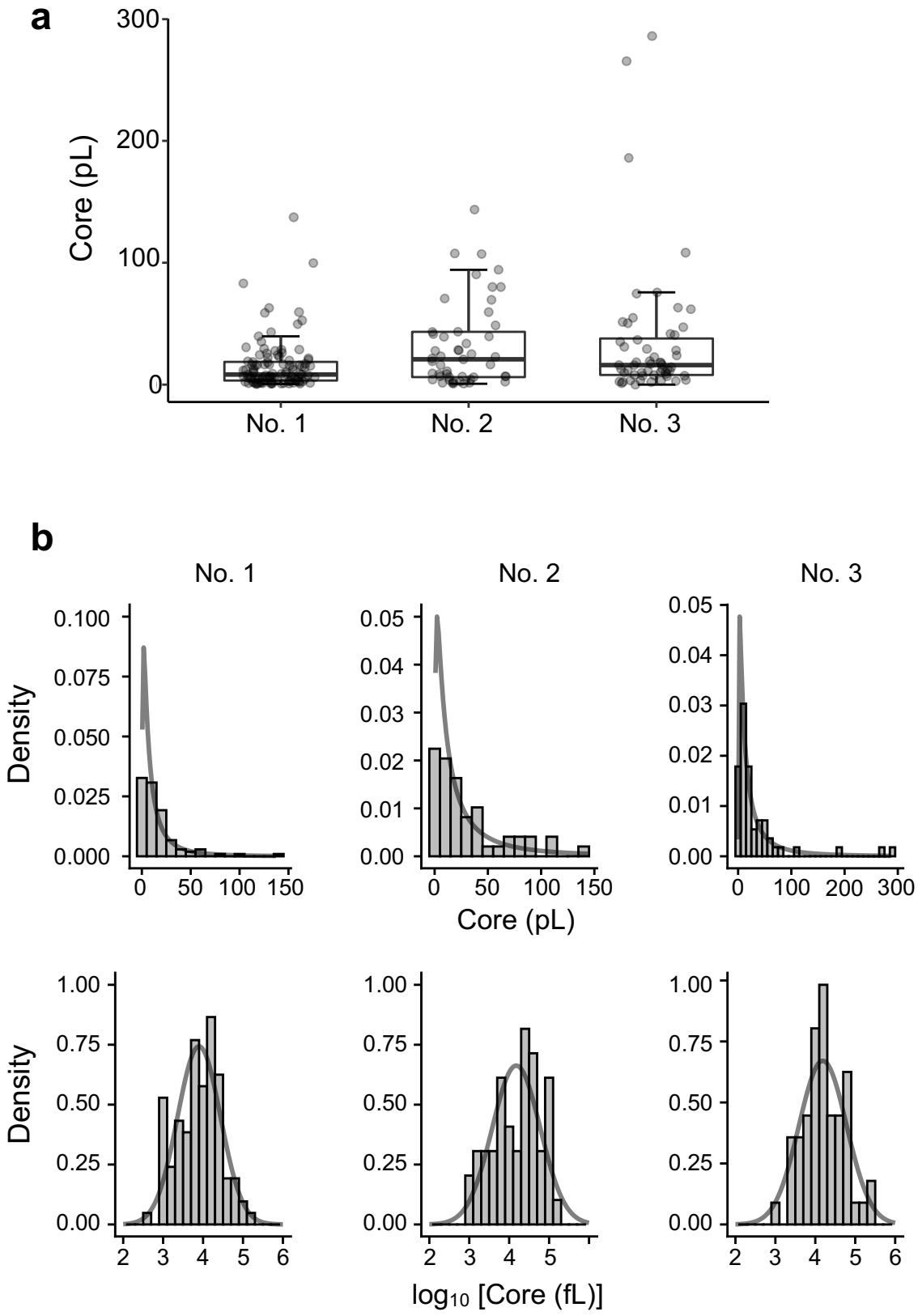
a
Core (pL)
300
200
100
0
No. 1
No. 2
No. 3
b
No. 1
No. 2
No. 3
Density
0.100
0.075
0.050
0.025
0.000
0.05
0.04
0.03
0.02
0.01
0.00
0
50
100
150
200
300
Core (pL)
1.00
0.75
0.50
0.25
0.00
2
3
4
5
6
log10 [Core (fL)]

Fig. 4

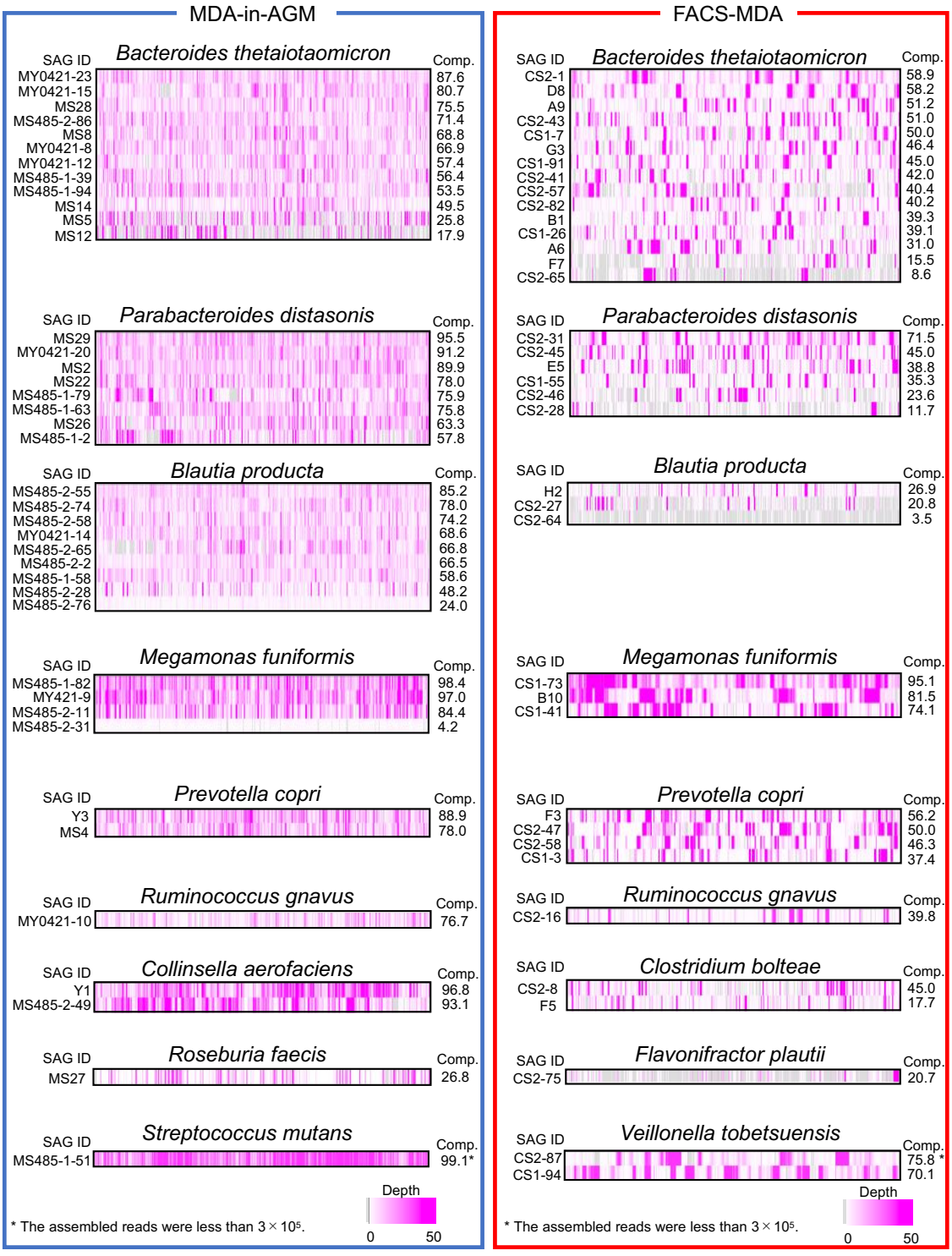
MDA-in-AGM
SAG ID
Bacteroides thetaiotaomicron
Comp.
MY0421-23 87.6
MY0421-15 80.7
MS28 75.5
MS485-2-86 71.4
MS8 68.8
MY0421-8 66.9
MY0421-12 57.4
MS485-1-39 56.4
MS485-1-94 53.5
MS14 49.5
MS5 25.8
MS12 17.9
Parabacteroides distasonis
MS29 95.5
MY0421-20 91.2
MS2 89.9
MS22 78.0
MS485-1-79 75.9
MS485-1-63 75.8
MS26 63.3
MS485-1-2 57.8
Blautia producta
MS485-2-55 85.2
MS485-2-74 78.0
MS485-2-58 74.2
MY0421-14 68.6
MS485-2-65 66.8
MS485-2-2 66.5
MS485-1-58 58.6
MS485-2-28 48.2
MS485-2-76 24.0
Megamonas funiformis
MS485-1-82 98.4
MY421-9 97.0
MS485-2-11 84.4
MS485-2-31 4.2
Prevotella copri
Y3 88.9
MS4 78.0
Ruminococcus gnavus
MY0421-10 76.7
Collinsella aerofaciens
Y1 96.8
MS485-2-49 93.1
Roseburia faecis
MS27 26.8
Streptococcus mutans
MS485-1-51 99.1*
Depth
0 50
* The assembled reads were less than 3 × 10⁵.
FACS-MDA
SAG ID
Bacteroides thetaiotaomicron
Comp.
CS2-1 58.9
D8 58.2
A9 51.2
CS2-43 51.0
CS1-7 50.0
G3 46.4
CS1-91 45.0
CS2-41 42.0
CS2-57 40.4
CS2-82 40.2
B1 39.3
CS1-26 39.1
A6 31.0
F7 15.5
CS2-65 8.6
Parabacteroides distasonis
CS2-31 71.5
CS2-45 45.0
E5 38.8
CS1-55 35.3
CS2-46 23.6
CS2-28 11.7
Blautia producta
H2 26.9
CS2-27 20.8
CS2-64 3.5
Megamonas funiformis
CS1-73 95.1
B10 81.5
CS1-41 74.1
Prevotella copri
F3 56.2
CS2-47 50.0
CS2-58 46.3
CS1-3 37.4
Ruminococcus gnavus
CS2-16 39.8
Clostridium bolteae
CS2-8 45.0
F5 17.7
Flavonifractor plautii
CS2-75 20.7
Veillonella tobetsuensis
CS2-87 75.8 *
CS1-94 70.1
Depth
0 50
* The assembled reads were less than 3 × 10⁵.

Fig. 5

73

74

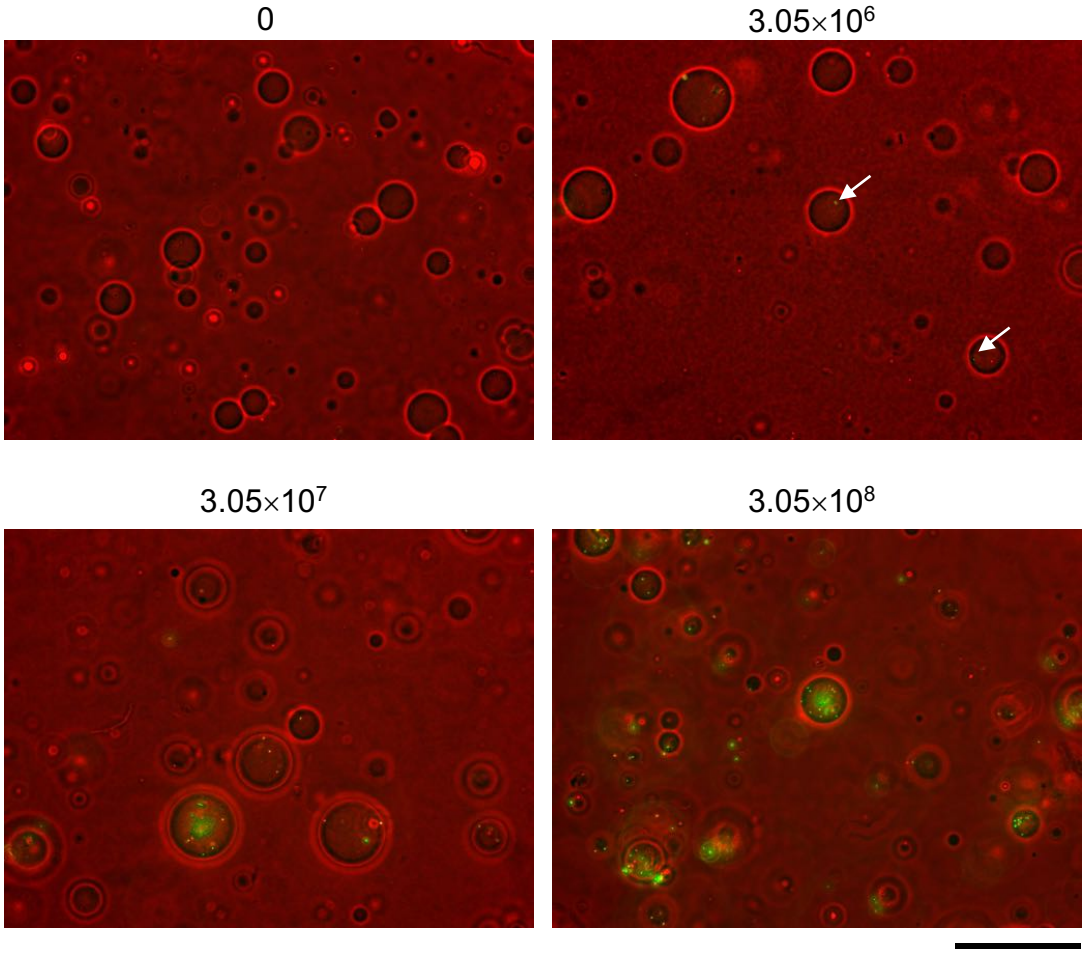

Fig. 6